

## CHARACTERIZATION OF PHOSWICH WELL DETECTORS FOR RADIOXENON MONITORING

Wolfgang Hennig<sup>1</sup>, Hui Tan<sup>1</sup>, William K. Warburton<sup>1</sup>, Anthony Fallu-Labruyere<sup>1</sup>, Konstantin Sabourov<sup>1</sup>,  
Justin I. McIntyre<sup>2</sup>, Matthew W. Cooper<sup>2</sup>, and Anshel Gleyzer<sup>3</sup>

XIA LLC<sup>1</sup>, Pacific Northwest National Laboratory<sup>2</sup>, and PhotoPeak, Inc<sup>3</sup>

Sponsored by National Nuclear Security Administration  
Office of Nonproliferation Research and Development  
Office of Defense Nuclear Nonproliferation

Contract No. DE-FG02-04ER84121

### **ABSTRACT**

Devices to measure the amount of radioactive xenon in the atmosphere have been installed in several locations around the world as part of the International Monitoring System to detect nuclear weapons testing. These devices extract small samples of xenon from large volumes of air and look for characteristic radioxenon isotopes emitting beta and gamma radiation in coincidence. To detect these coincidences, they currently employ a complex system of separate beta and gamma detectors which is very sensitive, but which requires careful calibration and gain matching of several detectors and photomultiplier tubes to achieve desired detection limits.

An alternative to separate beta and gamma detectors is the use of a single phoswich detector in which beta-gamma coincidences are detected by pulse shape analysis. The phoswich detector consists of a plastic scintillator (absorbing betas) optically coupled to a CsI(Tl) scintillator (absorbing gammas) and thus requires only a single photomultiplier tube and electronics readout channel, greatly simplifying setup and calibration. In this paper, we present the results from an experimental evaluation of two phoswich well detector prototypes, including energy resolution,

2-D beta/gamma energy histograms from a variety of test sources, and background count rates. From these measurements, we derive detector properties such as coincidence detection efficiency, background rejection and the ability to separate beta only, gamma only, and coincidence events. We will further discuss setup and calibration procedures and compare them to those for existing detector systems.

Report Documentation Page				Form Approved OMB No. 0704-0188	
Public reporting burden for the collection of information is estimated to average 1 hour per response, including the time for reviewing instructions, searching existing data sources, gathering and maintaining the data needed, and completing and reviewing the collection of information. Send comments regarding this burden estimate or any other aspect of this collection of information, including suggestions for reducing this burden, to Washington Headquarters Services, Directorate for Information Operations and Reports, 1215 Jefferson Davis Highway, Suite 1204, Arlington VA 22202-4302. Respondents should be aware that notwithstanding any other provision of law, no person shall be subject to a penalty for failing to comply with a collection of information if it does not display a currently valid OMB control number.					
1. REPORT DATE <b>SEP 2007</b>		2. REPORT TYPE		3. DATES COVERED <b>00-00-2007 to 00-00-2007</b>	
4. TITLE AND SUBTITLE <b>Characterization of Phoswich Well Detectors for Radioxenon Monitoring</b>				5a. CONTRACT NUMBER	
				5b. GRANT NUMBER	
				5c. PROGRAM ELEMENT NUMBER	
6. AUTHOR(S)				5d. PROJECT NUMBER	
				5e. TASK NUMBER	
				5f. WORK UNIT NUMBER	
7. PERFORMING ORGANIZATION NAME(S) AND ADDRESS(ES) <b>Pacific Northwest National Laboratory, PO Box 999, Richland, WA, 99352</b>				8. PERFORMING ORGANIZATION REPORT NUMBER	
9. SPONSORING/MONITORING AGENCY NAME(S) AND ADDRESS(ES)				10. SPONSOR/MONITOR'S ACRONYM(S)	
				11. SPONSOR/MONITOR'S REPORT NUMBER(S)	
12. DISTRIBUTION/AVAILABILITY STATEMENT <b>Approved for public release; distribution unlimited</b>					
13. SUPPLEMENTARY NOTES <b>Proceedings of the 29th Monitoring Research Review: Ground-Based Nuclear Explosion Monitoring Technologies, 25-27 Sep 2007, Denver, CO sponsored by the National Nuclear Security Administration (NNSA) and the Air Force Research Laboratory (AFRL)</b>					
14. ABSTRACT <b>see report</b>					
15. SUBJECT TERMS					
16. SECURITY CLASSIFICATION OF:			17. LIMITATION OF ABSTRACT <b>Same as Report (SAR)</b>	18. NUMBER OF PAGES <b>7</b>	19a. NAME OF RESPONSIBLE PERSON
a. REPORT <b>unclassified</b>	b. ABSTRACT <b>unclassified</b>	c. THIS PAGE <b>unclassified</b>			

## OBJECTIVES

As part of the International Monitoring System established by the Comprehensive Nuclear-Test-Ban Treaty, devices to measure the amount of radioactive xenon in the atmosphere have been installed in several locations around the world to detect nuclear weapons testing. These devices, one example being the Automated Radioxenon Sampler and Analyzer (ARSA) instrument developed at Pacific Northwest National Laboratory (Reeder, 1998), extract Xe from large volumes of air and then measure its radioactivity in an extremely low background counter. Since the Xe isotopes of interest all emit one or more beta particles or conversion electrons simultaneously with one or more gamma rays or X-rays, beta-gamma coincidence can be used effectively to suppress the natural background.

Currently, the devices use time based coincidence detection with separate detectors for beta and gamma radiation, which requires several channels of photomultiplier tubes (PMTs) and readout electronics. This leads to complex systems that require careful gain matching and calibration. Phoswich detectors have been studied as a potential simpler solution (Ely, 2003; Hennig et al., 2006-1), using pulse shape analysis (PSA) to detect coincidences in the signal from a single PMT. Using Monte-Carlo simulations, we previously studied several possible designs of phoswich well detectors that could be used as drop-in replacements for the existing ARSA detector unit (Hennig et al., 2006-2). The objective of the work presented in this paper was to build prototypes of the more promising designs and characterize their performance, i.e. determine properties such as energy resolution, coincidence detection efficiency, background rejection and the ability to separate beta only, gamma only, and coincidence events.

## RESEARCH ACCOMPLISHED

### Measurements

Two detector prototypes, named PW2 and PW3, were built. They both consist of a 1" diameter BC-404 plastic cell (absorbing betas) enclosed in and optically coupled to a 3" CsI(Tl) crystal (absorbing gammas), but differ in detector geometry as shown in Figure 1. PW2 is easier to manufacture, but due to the cut in CsI parallel to the PMT window, the light collection and thus energy resolution are degraded (Hennig et al., 2006-2). The geometry of PW3 has the best light collection and resolution among all designs studied in the simulations, but is more difficult to manufacture. The detector as currently built has a PMT with low gain and relatively high noise. Thus any results presented here for PW3 represent a detector that has not yet been fully optimized.

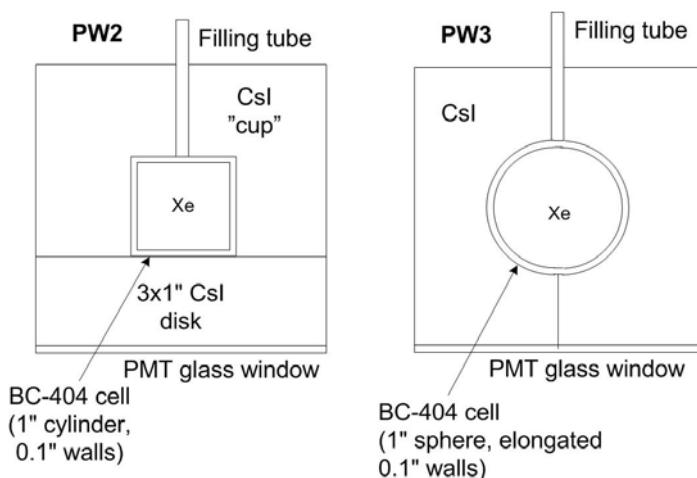


**Figure 1. Geometries of phoswich well detectors studied. Left: 1<sup>st</sup> well prototype (PW2); right: 2<sup>nd</sup> well prototype (PW3).**

### Energy Resolution

For PW2, we obtain an overall resolution of ~12% full width at half maximum (FWHM) for 662keV gamma rays from a <sup>137</sup>Cs source outside the detector. Closer analysis shows that there are actually 2 overlapping peaks with resolutions of ~7% and ~9% FWHM, their relative intensity varying according to location of the source. We

attribute this to the different light collection efficiency in the two sections of the CsI crystal (Hennig et al., 2006-2). For PW3, the resolution is ~9%, a single peak independent of the location of the source. Resolutions for other sources and energies are given in Table 1. Note that for low energies, the resolution of PW2 becomes equal to PW3, because the fixed ~6% separation of the 2 peaks from the two CsI crystal segments becomes negligible when added in quadrature with other peak broadening effects, such as photostatistics. Due to the noisy, low gain PMT currently used with PW3, its resolution is *worse* than PW2 at very low energies. These measurements will be repeated soon with a replaced PMT.

**Table 1. Energy resolution (FWHM) of PW2 and PW3. For external sources, no PSA to separate event types was applied. Values in () are preliminary results that need to be repeated with a replaced PMT.**

	PW2	PW3	Notes	ARSA (Reeder, 2004)
<b>Resolution at Ec = 662keV (external <sup>137</sup>Cs)</b>	12%	9%	PW2: two peaks, ~7% and ~9%	12%
<b>Resolution at Ec = 609keV (internal <sup>222</sup>Rn)</b>	12%	10%	Coincidence events only	
<b>Resolution at Ec = 120keV (external <sup>57</sup>Cs)</b>	16%	17%		22%
<b>Resolution at Ec = 60keV Ec = 29keV (external <sup>241</sup>Am)</b>	18% 31%	(23%) (36%)	PW3: small signal close to noise with this PMT	
<b>Resolution at Ec = 30keV Ep = 129keV (internal <sup>131m</sup>Xe)</b>	(36%) 29%	(48%)	Coincidence events only PW3: small signal close to noise with this PMT	32% 37%

### Energy Histograms

Using the fact that interactions in the plastic scintillator generate very fast pulses (< 100ns) while the CsI pulses are slow (several microseconds), each pulse from the phoswich detector is processed to extract the portion of energy deposited in CsI and plastic scintillators (Hennig et al., 2006-1). Figure 2 shows 2D histograms of CsI energy (Ec) vs. plastic energy (Ep) for measurements with a <sup>222</sup>Rn source (NIST SRM 4974). The 2D histograms show horizontal lines of coincidence events from beta particles (Ep varies) and photons (peaks at Ec = 80keV, 241keV, 295keV, 351keV and 609keV) from <sup>222</sup>Rn daughter products. The 80keV line is offset in Ep as a conversion electron with constant energy emitted at the same time as the variable energy beta particle. The energy resolution of Ec for the 609keV coincidence line is about 11.8% FWHM in PW2, with a noticeable shoulder or second peak towards higher energies (see Figure 3). For PW3, the resolution is about 10.2% with no shoulder.

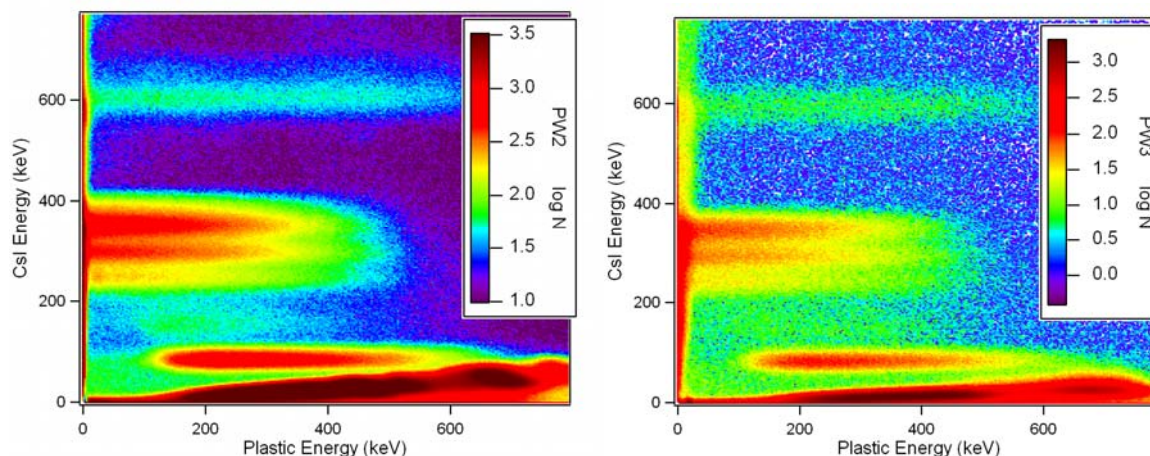


**Figure 2.** 2D energy histograms for PW2 (left) and PW3 (right) for measurements with a  $^{222}\text{Rn}$  source. Note the color scales differ due to different number of counts in each measurement.

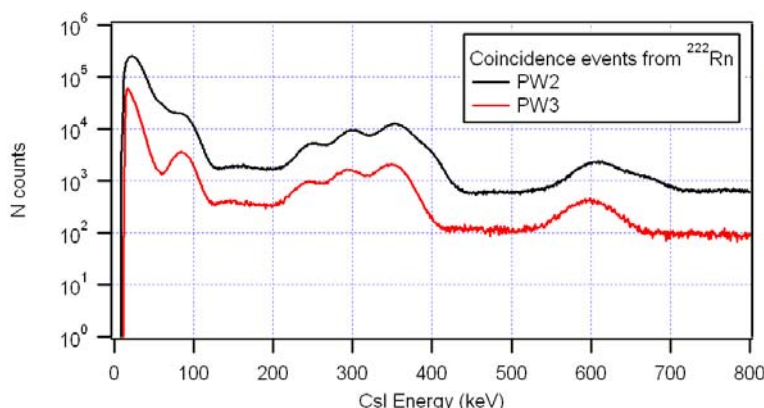


**Figure 3.** Histograms of energy deposited in CsI (in coincidence events only) for PW2 and PW3 in measurements with a  $^{222}\text{Rn}$  source. The shoulders in the peaks of PW2 at 400 and 670 keV are due to the non-uniform light collection in different sections of the detector.

In both detectors, but less pronounced in PW3, there is also a rising diagonal line starting at  $E_c \sim 0\text{keV}$ ,  $E_p \sim 150\text{keV}$ . The “peaks” along the line—allowing for a different energy scale and non-linearity at low energies for heavy charged particles (Knoll, 2000)—match the alpha energies in the  $^{222}\text{Rn}$  decay chain. We thus conclude that these events are alpha particles, generating a slightly different pulse shape (slower decay) than electrons or photons when interacting with the plastic scintillator. The PSA algorithms, in their current form, interpret the slower decay as a contribution of a slow CsI pulse and thus compute a component in  $E_c$  proportional to the pulse height. Because Rn is removed from the sample to minimize interference in the 80keV line in Xe monitoring measurements, there should then be no significant interference from alpha particles either. On the other hand, it is also possible to modify the PSA algorithms to detect and remove alpha pulses from the recorded data, e.g., by shape-matching fits, measuring the fall time or additional sums over characteristic intervals in the pulse.

Figure 4 shows a 2D histogram of  $E_c$  vs.  $E_p$  for measurements with a  $^{131\text{m}}\text{Xe}$  source. The 2D histogram has one coincidence peak due to 30keV X-rays in coincidence with 129keV conversion electrons and a plastic only peak at  $\sim 160\text{keV}$  from conversion electrons that are not in coincidence. The resolution for coincidence events for PW2 is  $\sim 29\%$  at  $E_p = 129\text{keV}$ . In measurements with a mixture of  $^{131\text{m}}\text{Xe}$  and  $^{133\text{g}}\text{Xe}$ , the resolution at  $E_c = 30\text{keV}$  is  $\sim 36\%$  for PW2 and  $\sim 48\%$  for PW3.

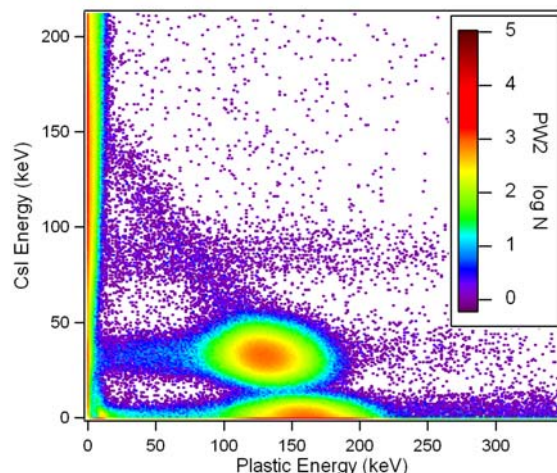


**Figure 4. 2D energy histograms for PW2 for measurements with a  $^{131m}\text{Xe}$  source. The 80keV line comes from traces of other sources ( $^{222}\text{Rn}$  or  $^{133}\text{Xe}$ ). Measurements for PW3 are still in progress.**

**Background:** In monitoring applications, the samples of radioxenon collected are very small, so the background count rate of the detector has to be as small as possible. In a lead enclosure (lead wall thickness is 2" with an additional 0.5" inner lining with Oxygen-Free High Conductivity [OFHC] copper), we measure an overall rate of 4-5 counts/s for PW2, of which ~0.05 counts/s are coincidences. The overall rate for PW3 is 3-7 counts/s, of which ~0.04-0.09 counts/s are coincidences. The ARSA detector, consisting of two much bigger NaI crystals, has an overall background rate of ~30 counts/s of which 0.1 counts/s are coincident, i.e., the background in Xe regions of interest is can be up to a factor of 2 higher.

## Characterization

### Coincidence Detection Efficiency

The coincidence detection efficiency at a given energy is defined as the number of net coincidence counts in the peak, divided by the number of all net counts in the peak. From the  $^{131m}\text{Xe}$  measurement for PW2, we obtain the coincidence detection efficiency for the 30keV peak as 97.6%. A small fraction (about 1.5%) of coincidence events fall outside the main peak, due to two processes: 1) Conversion electrons pass through the plastic and reach the CsI, i.e., a portion of the conversion electron's energy is deposited in the CsI and added to the measured X-ray energy. This creates the diagonal line to the upper left from the main peak in the histogram. 2) Conversion electrons lose some of their energy in passive parts of the detector, i.e., a portion of the conversion electron's energy is lost. This causes the horizontal line to the left from the main peak. For a given conversion electron energy, the fraction of such events depends primarily on the wall thickness of the plastic cell (Hennig et al., 2006–2).

Measurements with a mixture of  $^{131m}\text{Xe}$  and  $^{133g}\text{Xe}$  result in an estimated coincidence detection efficiency of 98.5% for PW2 and 98.9% for PW3. As expected, the values are very similar since the difference in detector design affects mostly the light collection, not the absorption of radiation.

### Background Rejection

Adding an external  $^{137}\text{Cs}$  source as “controlled background” in measurements with PW2 in the lead enclosure, we find an increase in overall count rate of 77 counts/s (with this particular source). Most of the  $^{137}\text{Cs}$  photons interact only with the CsI; however a small fraction will Compton scatter from the CsI to the plastic or vice versa, generating coincidence events. The increase in the coincidence count rate is only 0.48 counts/s, i.e. 0.6% of the overall increase. Thus the background rejection rate (background represented by a  $^{137}\text{Cs}$  source) is 99.4% for PW2. For PW3, we compute a background rejection rate of 99.2% from a measurement with a source adding 526 counts/s.

### Ability to Separate Event Types

Events are processed one by one with PSA algorithms to categorize them as CsI only (gamma), plastic only (beta) or both (coincidence) based on user defined thresholds in energy and signal rise time. Close inspection of a subset of events indicate an error rate of ~1% in each category due to the automated pulse shape analysis, for example 1% of the events categorized as coincidence events are actually CsI only events or plastic only events. The most common reasons for mis-categorization are noise spikes in very low energy events and random coincidences (e.g., 2 plastic pulses following each other closely), and most of the mis-categorized events thus fall close to the origin in the 2D histogram, outside the region of interest for Xe isotopes.

From the resolution of the coincidence peak and the distribution of beta only and gamma only events along the axes in the 2D histogram, we estimate the minimum detectable coincidence energy for PW2 to be  $E_c \sim 13\text{keV}$  and  $E_p \sim 25\text{keV}$  in the plastic, which means that lower energies are not clearly distinguishable from CsI only or plastic only events, respectively. A setup using separate, optically isolated detectors with typical thresholds may have a minimum detectable coincidence energy of  $E_c \sim 14\text{keV}$  and  $E_p \sim 5\text{keV}$ , but no radioxenon coincidences of interest occur at such low energies.

### Calibration

Quantitative isotope analysis for radioxenon monitoring relies on measuring the number of counts in specific regions of interest in the 2D histogram. Therefore, in repeated measurements and over long periods of time, the detector system has to deliver spectra with a fixed range in both beta energy and gamma energy (exact same scale keV/bin).

For a single detector (one scintillator with PMT), the deposited energy can be assumed to be proportional to the measured pulse height, and thus a single gain calibration constant is usually sufficient to histogram pulses into an energy spectrum. However, even when holding external environmental factors such as temperature and magnetic field constant, gain may drift over time. Therefore the calibration constant has to be verified periodically and either the constant or the PMT gain has to be adjusted to correct for any gain changes.

In the phoswich detector system, the plastic and CsI energies are derived by PSA algorithms from the measured pulse height (called E) and a sum accumulated over the initial portion of the pulse (called P). Both E and P depend on the gain of the detector as in a single detector. The algorithms rely on two processing constants, essentially the ratios P/E for plastic only and CsI only events. These ratios are detector constants depending on the pulse shape and relative light output of the plastic and CsI scintillators. They are easily determined in calibration measurements with beta/gamma emitting reference sources such as  $^{222}\text{Rn}$  and  $^{131\text{m}}\text{Xe}$ , but even an external  $^{137}\text{Cs}$  source generates in a few minutes a sufficient number of plastic only pulses for the calibration. Most importantly, the P/E ratios *do not* depend on the gain of the detector, since both fast and slow components of the pulse are equally affected by any gain changes. This can be seen in Figure 5 (left), plotting the P/E ratios and the position of the 662keV peak from  $^{137}\text{Cs}$  as a function of PMT bias (i.e., gain). While the peak position shifts to higher bins at higher gains, the P/E ratios remain constant (the standard deviation of measured P/E ratios is 0.5% for the plastic scintillator and 0.2% for CsI). Consequently, in measurements with different gains, the energy scales of  $E_p$  and  $E_c$  both change by the same factor. The slope fitted to the Compton scattered events in the 2D histogram—the light blue line in Figure 5 (right)—remains a constant within the precision of the measurement.

In practice this means that even though the PSA introduces additional processing constants to determine the individual energies, only the overall gain calibration has to be verified and adjusted periodically. The processing constants have to be determined only once, for example at the production or installation of the detector. In periodic adjustments for gain, only a single measurement with a  $^{137}\text{Cs}$  reference source, as simple as determining the peak position of the 662keV peak, is required to calibrate the scales of both energy axes. Alternatively, if there are well-defined peaks in the naturally occurring singles background, they might also be used to monitor and stabilize the PMT's gain.



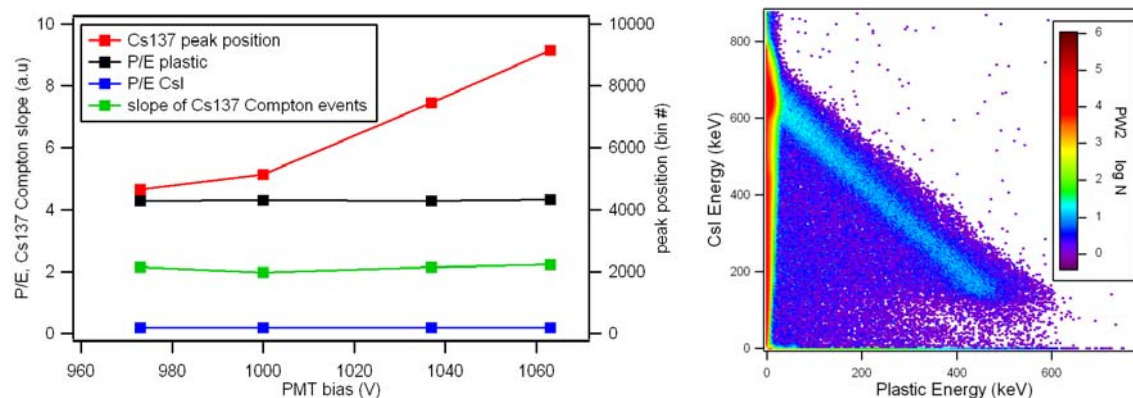


**Figure 5. Left: Variation of peak position and processing constants with PMT bias (i.e., gain). Right: 2D energy histogram for a  $^{137}\text{Cs}$  source. The slope of the full energy Compton events (line of light blue pixels) is plotted in green in the left graph for different values of PMT bias.**

In contrast, the existing ARSA detector system has separate beta and gamma detectors and uses multiple PMTs to read out the same scintillator. Therefore, during calibration these shared PMTs first have to be adjusted to have the exact same gain, and then for each scintillator a gain calibration constant has to be determined. This amounts to 6 gain matches and 6 gain constants for 4 sample cells compared to only 1 gain dependent calibration constant per sample cell for the phoswich detector. The resulting simplifications in field operation that are expected to result from this reduction in necessary calibration measurements have, naturally, been a major driving force for the development of this phoswich technology.

### **CONCLUSIONS AND RECOMMENDATIONS**

In summary, we have built and evaluated two phoswich well detector prototypes. Overall, their performance is comparable to that from the existing ARSA detector: the background is somewhat lower, the resolution slightly better or equal, and the energy thresholds for coincidence detection somewhat higher. PW3 has better energy resolution, as expected from previous simulations, but more tests are necessary with a better PMT to complete its evaluation. The key advantage of the phoswich detectors is their much simpler calibration, since the single PMT requires only periodic calibration of one gain dependent constant per sample cell instead of three, and the beta energy can be scaled from the peak position of the  $^{137}\text{Cs}$  gamma peak. Future work will include the production and long term evaluation of two additional phoswich detectors made in the same geometry as PW3.

### **REFERENCES**

- Ely, J. H., C. E. Aalseth, J. C. Hayes, T. R. Heimburger, J. I. McIntyre, H.S. Miley, M. E. Panisko, and M. Ripplinger (2003). Novel Beta-Gamma coincidence measurements using phoswich detectors, in *Proceedings of the 25th Seismic Research Review—Nuclear Explosion Monitoring: Building the Knowledge Base*, LA-UR-06-6029, Vol. 2, pp. 533–541.
- Hennig, W., H.Tan, W. K. Warburton, and J. I. McIntyre (2006). Single channel beta-gamma coincidence detection of radioactive Xenon using digital pulse shape analysis of phoswich detector signals, *IEEE Transactions on Nuclear Science* 53: (2) p. 620.
- Hennig, W., H.Tan, A. Fallu-Labruyere, W. K. Warburton, J. I. McIntyre and A. Gleyzer (2006). Design of a phoswich well detector for radioxenon monitoring, in *Proceedings of the 28th Seismic Research Review: Ground Based Nuclear Explosion Monitoring Technologies*, LA-UR-06-5471, Vol. 2, pp. 801–810.
- Knoll, G. F. (2000) *Radiation Detection and Measurement*, J Wiley & Sons, Inc. Chapter 8.
- Reeder, P. L., T.W. Bowyer, and R. W. Perkins, (1998). Beta-gamma counting system for Xe fission products, *Journal of Radioanalytical and Nuclear Chemistry* 235: (1–2), 89–94.
- Reeder, P. L., T.W. Bowyer, J. I. McIntyre, W.K. Pitts, A. Ringbom, and C. Johansson (2004). Gain calibration of  $\beta/\gamma$  coincidence spectrometer for automated radioxenon analysis., *Nuclear Instruments and Methods in Physics Research A* 52, 586–599.